Eur Biophys J (2009) 38:793–806
DOI 10.1007/s00249-009-0474-5

ORIGINAL PAPER

Spatial allelic imbalance of *BCL2* genes and chromosome 18 territories in nonneoplastic and neoplastic cervical squamous epithelium

Thorsten Wiech · Stefan Stein · Victoria Lachenmaier · Eberhard Schmitt · Jutta Schwarz-Finsterle · Elisabeth Wiech · Georg Hildenbrand · Martin Werner · Michael Hausmann

Received: 27 February 2009 / Revised: 1 May 2009 / Accepted: 4 May 2009 / Published online: 3 June 2009

Abstract Several studies suggest a correlation between genome architecture and gene function. To elucidate mechanisms of gene positioning during cell differentiation and malignant transformation we investigated the nuclear positions of the *BCL2* alleles and chromosome 18 territories in different layers of nonneoplastic cervical squamous epithelium and cervical squamous carcinomas in relation to gene expression. Fluorescence in situ hybridization and three-dimensional (3D) image analysis using tissue sections revealed that one *BCL2* allele was located more peripherally than the other one in nuclei of the basal layer of nonneoplastic epithelium. During terminal cell differentiation the outer *BCL2* allele showed a shift towards the nuclear center. In BCL2-expressing carcinomas the inner *BCL2* allele was located more peripherally compared with the basal layer of nonneoplastic epithelium. Our results suggest a functional relevance of unequal allelic *BCL2* gene positioning and support the hypothesis that transcriptional *BCL2* activation is associated with *BCL2* relocation towards the nuclear periphery.

Keywords *BCL2* gene domains · Chromosome 18 territories · 3D FISH · Gene regulation · Genome architecture · Cervical cancer

This article has been submitted as a contribution to the festschrift entitled "Uncovering cellular sub-structures by light microscopy" in honor of Professor Cremer's 65th birthday.

T. Wiech · V. Lachenmaier · E. Wiech · M. Werner (✉) · M. Hausmann
Institute of Pathology, University Hospital Freiburg, Breisacher Strasse 115a, 79106 Freiburg, Germany
e-mail: direktion-pathologie@uniklinik-freiburg.de

S. Stein · E. Schmitt · J. Schwarz-Finsterle · G. Hildenbrand · M. Hausmann
Kirchhoff Institute of Physics, University of Heidelberg, Im Neuenheimer Feld 227, 69120 Heidelberg, Germany

Introduction

Special arrangement patterns of hetero- and euchromatin within the interphase nucleus, such as radiating chromatin of plasma cells, coarsely granular chromatin of cancer cells, and a "salt-and-pepper" chromatin pattern of neuroendocrine tumor cells, are well-established histopathological diagnostic features that indicate correlation between genome architecture and cellular function or differentiation. Sequence specific labeling of DNA using fluorescence in situ hybridization (FISH) (Cremer et al. 2008) and optical sectioning with 3D image analysis confirmed that the spatial arrangement of the human genome in the interphase nucleus is nonrandom and follows a functionally correlated motion (Bolzer et al. 2005; Cremer and Cremer 2001; Cremer et al. 2000, 2006; Kozubek et al. 2002; Kosak et al. 2007; Lanctôt et al. 2007). Each chromosome occupies a distinct volume within the nucleus—the chromosome territory—which can be subdivided into subchromosomal domains, forming surface irregularities, which more or less intermingle with neighboring territories (Albiez et al. 2006; Branco and Pombo 2006). The intranuclear position of territories and individual genes described by the relative radial distance to the nuclear center is nonrandom and seems to follow special rules; for instance, a correlation of chromosome position and gene density (Kupper et al. 2007) has been shown to be evolutionary conserved (Tanabe et al. 2002; Neusser et al. 2007), and gene positioning has been shown to depend on their transcriptional status (Kosak and Groudine 2004; Dundr et al.

2007; Sexton et al. 2007). Relative chromosome positioning is preserved within one cell type (Parada et al. 2002) independently of the individual, as has also been reported for nonneoplastic pancreatic and breast ductal epithelium (Wiech et al. 2005). In addition, the shape of chromosome territories seems to vary little, as indicated by the small variance of roundness of chromosome 8 territory in pancreatic ductal epithelium (Wiech et al. 2005).

However, imaging of living cells revealed that chromatin in interphase nuclei is dynamic in structure and nuclear position up to a certain level (Abney et al. 1997; Zink et al. 1998; Lanctôt et al. 2007). Spatial repositioning of DNA regions seems to play a role in regulation of gene expression. Several studies suggest that transcriptional activation of genes in lymphocytes and adenocarcinoma cells correlates with a repositioning towards the nuclear interior (Kosak et al. 2002; Zink et al. 2004), away from the constitutional heterochromatin (Hewitt et al. 2004). Vice versa, gene silencing has been shown to be associated with spatial proximity to heterochromatin (Bartova et al. 2002; Harmon and Sedat 2005). In contrast, investigations in *Saccharomyces cerevisiae* suggest an association between gene activation and repositioning of the locus towards the nuclear periphery (Casolari et al. 2004), in proximity to nuclear pores in order to serve to optimally express the gene (Soutoglou and Misteli 2007). These inconsistent findings may reflect the complexity of interactions that may be involved in regulation of transcription, such as colocalization of genes on different chromosomes, several genes sharing the same transcription factory, various activating or repressing factors, the genomic context of the respective locus, and other factors.

Spatial genome organization has mostly been studied in monolayer cell cultures. However, the findings cannot be transferred directly into tissues, since the same cell type in monolayer cultures and tissues show differences in nuclear structure. Moreover, there are interactions between the extracellular matrix and the architectural organization of the nucleus (Lelievre et al. 1998) which can only be assessed in tissue. Application of 3D FISH methods in paraffin tissue sections preserves the natural microanatomical context, allowing correlation studies between intranuclear genome architecture and tissue texture, cellular positioning or extracellular structures. Furthermore, in several tissues, for example, colonic crypt epithelium or squamous epithelium, there is a well-defined spatial direction of terminal cell differentiation, so that the cellular position in a tissue section provides an indication about the respective cell differentiation status.

Expression of apoptosis-related genes requires tight regulatory mechanisms in cell differentiation, which may be impaired in neoplastic transformation and autoimmune or degenerative diseases (Cory and Adams 2002). The "intrinsic" or "stress" pathway of cell death is primarily regulated by members of the BCL2 family, which are subject to several transcriptional and posttranslational control mechanisms (Adams and Cory 2007). Immunohistochemical staining reveals a decrease of BCL2 expression in normal squamous epithelium towards the surface. In addition to prolonged cell survival by inhibition of apoptosis, BCL2 can also promote genomic instability by affecting DNA repair capacity (Youn et al. 2005). It has been found to be upregulated in 54% of invasive cervical cancer and in 68% of preinvasive cervical intraepithelial neoplasia (CIN) by immunohistochemical staining (Ozalp et al. 2002), as well as in lymph node metastases of cervical cancer, as detected by expression profiling (Hagemann et al. 2007).

Thus, we investigated the expression-related intranuclear radial position of chromosome 18 territories and the orientation of *BCL2* genes in normal terminal differentiation of squamous epithelium in the vaginal part of uterine cervix in reference to the nuclear center. Incorporating analyses of BCL2-overexpressing as well as BCL2-non-overexpressing cervical squamous cell carcinomas, our study provides new aspects of genome architecture in nonneoplastic and neoplastic cells within their natural histological context in association with gene expression.

Materials and methods

Tissue microarrays and immunohistochemistry

Tissue microarrays were prepared from routinely overnight formalin-fixed (4% formaldehyde in phosphate-buffered saline, PBS) and paraffin-wax-embedded human tissue specimens, using 2-mm cores. Cylinders of six specimens of nonneoplastic ectocervical squamous epithelium (NNSE) and four invasive cervical squamous carcinomas (SCC) were punched from preselected areas and transferred into a recipient paraffin block. The carcinomas have been classified as moderately differentiated, nonkeratinizing invasive cervical squamous cell carcinomas, according to World Health Organization (WHO) classification schemes (Wells et al. 2003). Tumor stages T1b1 and T1b2, according to the International Union against Cancer (Sobin and Wittekind 2002) were represented. For hematoxylin/eosin and immunohistochemical staining 2-µm-thick sections were prepared. Immunohistochemistry was performed with anti-human BCL2 oncoprotein monoclonal mouse antibody (DAKO, Glostrup, Denmark, clone 124, diluted 1:1,000) using Dako REAL^{TM} Detection System, Alkaline Phosphatase/RED-labeled rabbit anti-mouse antiserum, according to the DAKO standard protocol. The slides were pretreated in a steamer for 30 min (pH 9.9). The staining

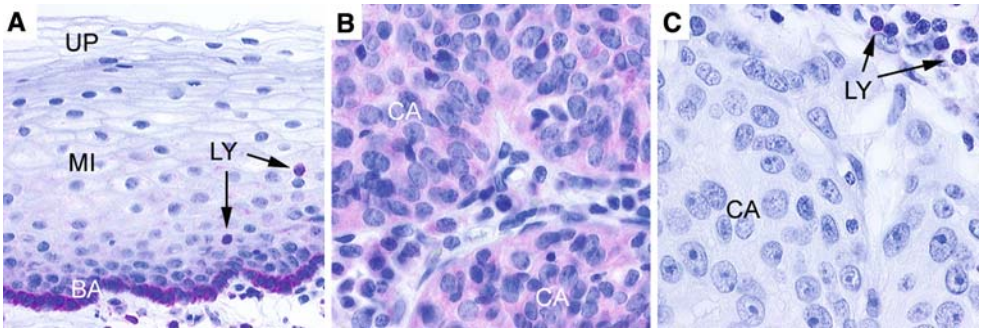

Fig. 1 Immunohistochemical staining for BCL2: **a** (100× magnification) Abundant cytoplasmic positivity in the basal layer (*BA*), weak protein expression in parabasal and middle layers (*MI*), and no detectable expression in the upper layers (*UP*) of nonneoplastic cervical squamous epithelium; note two BCL2-positive intraepithelial lymphocytes (*LY*). **b** (200× magnification) Section of a BCL2$^+$ squamous cell carcinoma of the cervix (*CA*). **c** (200× magnification) Section of a BCL2$^-$ squamous cell carcinoma of the cervix (*CA*). Note the BCL2-positive lymphocytes (*LY*) in the stroma in the right upper corner as an internal positive control

intensity of the nonneoplastic and neoplastic epithelial cells was compared with the staining intensity of lymphocytes, which were present in the subepithelial connective tissue in every case and served as internal positive control. Staining intensity was semiquantitatively graded as strong, weak or negative.

Fluorescence in situ hybridization (FISH)

For FISH analysis, tissue microarray sections (15 μm) were cut and mounted on glass slides. Locus-specific probes for *BCL2*, labeled with SpectrumGreen (kindly provided by Prof. Dr. R. Siebert, Institute of Human Genetics, University Hospital Schleswig-Holstein, Kiel, Germany) and whole chromosome painting (WCP) probes for visualization of the chromosome 18 territory labeled with SpectrumOrange (Abbott Molecular Diagnostics), were used.

Paraffin was removed by xylene (30 min) and isopropanol (3 min) and the slides were hydrated in a graded series of ethanol (100%, 96%, 70%, and 50%) and PBS (pH 7). Pretreatment [20 min in a microwave oven (180 W) in citrate buffer, pH 6, and pronase E (0.05%) digestion for 3 min at 37°C] was performed. After washing in PBS, the slides were denatured in 70% formamide for 15 min at 75°C. The slides were dehydrated over a graded series of ethanol (70%, 90%, 100%, at −20°C) and air-dried. The FISH probes were added onto the slides and incubated for 48 h at 37°C. After hybridization and nuclear counterstaining with Hoechst 33342 (Molecular Probes) for 10 min, the slides were placed in 2× SSC/0.1% NP-40 (7.4) at 73°C for 2 min, embedded in antifade solution (Vectashield), and covered with a standard cover glass.

Fluorescence microscopy and image acquisition

Since NNSE shows strong BCL2 immunohistochemical staining of the basal layer, weak staining of the middle third, and no staining of the apical cells (Fig. 1a), these three groups (basal/middle/upper layer) were defined as stages in a model of terminal cell differentiation. Two invasive cervical SCC with strong BCL2 staining ($n = 2$, both nonkeratinizing, grade 2, T1b1) represented the group of BCL2-positive carcinomas (SCC BCL2$^+$) (Fig. 1b), and two SCC without BCL2 expression ($n = 2$, both nonkeratinizing, grade 2, T1b1 and T1b2) were taken as the group of BCL2-negative carcinomas (SCC BCL2$^-$) (Fig. 1c).

Three-dimensional image stacks (voxel size 102 × 102 × 325 μm^3) were acquired using a Zeiss Axioplan2 imaging microscope (Carl Zeiss Jena, Jena, Germany) equipped with a PlanApochromat 63×/NA1.4 oil objective lens and the ApoTome (Carl Zeiss Jena) for optical sectioning (for details, see Wiech et al. 2005). The image stacks in the three color planes (red for SpectrumOrange, green for SpectrumGreen, and blue for DAPI) were recorded sequentially (Fig. 2). For false-color visualization and experiment control, 3D views were reconstructed by the AxioVision software. TIFF image stacks were exported for interactive object segmentation of nuclei and labeled sites using ImageJ image-processing software. The cell nuclei were selected according to 3D completeness and clearly visible FISH signals.

A total of 121 nuclei of the three groups of NNSE (basal $n = 45$, middle $n = 39$, upper layer $n = 37$) and 82 nuclei of the four carcinomas (SCC BCL2$^+$ $n = 44$, SCC BCL2$^-$ $n = 38$) were appropriate for further quantitative analysis.

Three-dimensional image analysis

The TIFF images of the presegmented cell nuclei were converted into kdf format and further evaluated as described in detail elsewhere (Stein 2006; Schmitt et al. manuscript in preparation). Briefly, to increase the signal-to-noise ratio, the images were first processed by 3 × 1 × 1 and 1 × 3 × 1 or 5 × 1 × 1 and 1 × 5 × 1 binomial filters

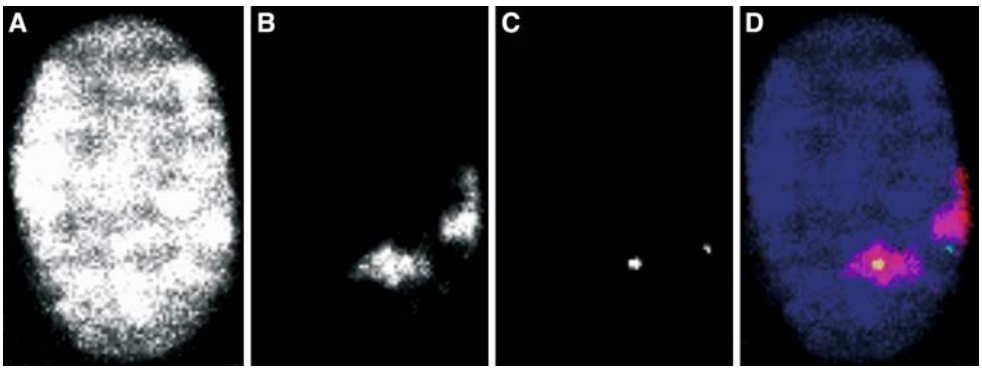

Fig. 2 Example of a segmented basal cell of nonneoplastic squamous epithelium (*NNSE*) with **a** Hoechst 33258 nuclear counterstain, **b** whole chromosome painting for visualization of the chromosome 18 territories, and **c** locus-specific hybridization of the *BCL2* gene domains, **d** the merged picture of all three channels reveals interchromosomal differences of intranuclear positioning of the territories and the *BCL2* genes

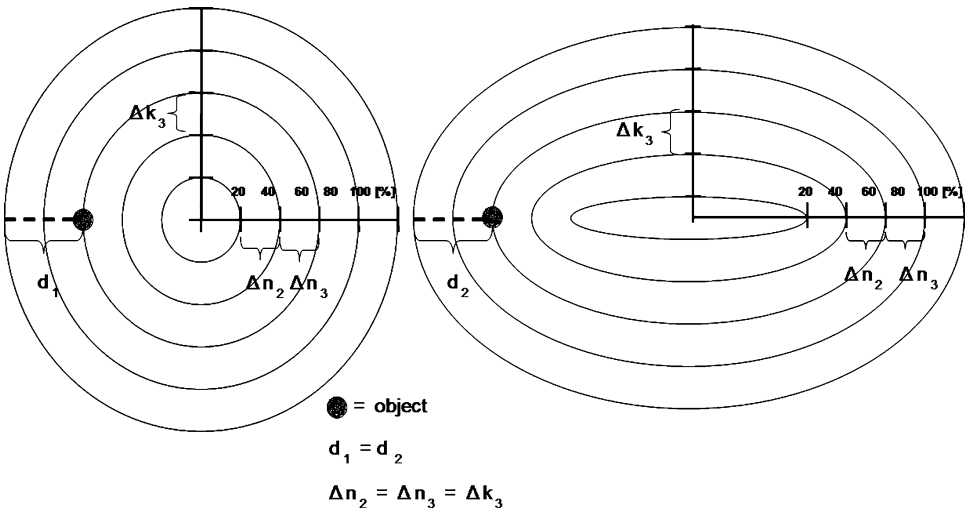

Fig. 3 Schematic representation of the radial segments of a cell nucleus equidistantly following the nucleus border. For simplicity only five shells with width Δn_i are shown. d is the Euclidean distance of the object to the nuclear border. Comparison of the left image (*spheric cell nucleus*) with the right image (*ellipsoid cell nucleus*) indicates that the chosen description of the nuclear shells can be used independently of the nuclear shape

and the background was reduced by a threshold in the grayvalue histogram. For the segmentation of the cell nuclei and the chromosome territories an iterative threshold procedure (isodata procedure) was applied. The domains of the *BCL2* genes were segmented by means of a top-hat algorithm. Centers and borders of nuclei were automatically determined by analyzing the 3D image stack of the Hoechst counterstain. From the segmented chromosome territories and gene domains the intensity barycenters were calculated.

For the calculation of the relative radial position (%) of the respective genome element highlighted by a DNA specific fluorescence label, the shortest Euclidean distance d to the nuclear border of every voxel x of the cell nucleus was calculated by

$$d = \sqrt{(x_1 - y_1)^2 + (x_2 - y_2)^2 + (x_3 - y_3)^2}$$

with x_i and y_i being the three-dimensional coordinates of the voxel x and the border voxel y, respectively. The distance d was normalized to the maximum shortest Euclidean distance. In the case of ellipsoidal cell nuclei this corresponds to the short axis of the ellipsoid (Fig. 3, right image). By multiplication of this normalized distance with an appropriate scaling factor, the cell nucleus was subdivided into ten equal segments of width Δn_i to the nucleus surface (Fig. 3). Using the same algorithm, the chromosome 18 territories were subdivided into shells for comparing the relative distances of the *BCL2* alleles with respect to the territories. In order to determine the radial positions of nuclear elements of a certain cell type the position of the intensity barycenter within these shells was calculated and given as a percentage relative to the nuclear center (Fig. 3). In this way, possible systematic difference of 3D parameters due to changes of nuclear shape, especially in the upper layer of epithelium in which nuclei tend to appear ellipsoid or flat rather than round, could be reduced to a minimum (compare left and right image in Fig. 3).

The sum of the voxel intensities measured in all evaluated nuclei per set was set to 100% for each color channel for normalization. The cumulative relative DNA content of the shells was displayed as a function of the relative distance r from the determined center of the nucleus or territory, respectively. Radial positions of territories in reference to the nuclear center, of *BCL2* genes in reference to the territorial center, and of *BCL2* genes in reference to the nuclear center were illustrated in this way (Fig. 4).

In addition to the radial positions the absolute distances (in microns) of the homologous elements were calculated. In order to compare the distances independently of the nuclear size the cell nuclei were transformed into a unit sphere with radius $R = 1$. The normalized distances of the nuclear elements refer to this unit sphere and are given in units of R (Fig. 5).

All parameters were determined by analyzing both chromosome 18 territories or both alleles of *BCL2* per cell, respectively, and then by analyzing the inner, more central, and the outer (more peripheral) chromosome territory 18 or *BCL2* allele separately.

Statistical analysis

To distinguish between significantly different radial positions and distances of chromosome territories and gene domains, statistical tests were applied to the complete distributions of the respective measurements rather than to their mean values alone. The analysis was applied to the distance data for the *BCL2* gene domains as well as to the chromosome 18 territories as a whole in reference to the nuclear center (normalized relative radial positioning), to the distance from the *BCL2* gene domain to the chromosome 18 territory, to the distance and normalized distance of the homologous chromosome territories, and to the distance and normalized distance of the homologous *BCL2* gene domains. The five distributions of the measurements for NNSE basal layer, NNSE middle layer, NNSE upper layer, SCC BCL2$^+$, and SCC BCL2$^-$ were compared. In addition to the overall analysis, relations between inner and outer *BCL2* alleles and inner and outer chromosome 18 territories were also inspected separately. Statistically significant differences were tested by the two-sided Kolmogorov–Smirnov two-sample test (KS test) (Sokal and Rohlf 1981) using the analytical representation for the critical values. As we do not have indications for normal distributions of the respective measurements, we decided to use this nonparametric test, the null hypothesis of which is identity in distribution for the two samples. The test is known to be sensitive to differences also of higher moments of the distributions, such as dispersion and skewness. The results for the KS test are shown using the significance value α. All values clearly above $\alpha = 0.15$ were assumed to be insignificant.

Results

Immunohistochemistry

Immunohistochemical staining of the nonneoplastic squamous epithelium revealed abundant cytoplasmic positivity for BCL2 in the basal layer, weak staining of the middle third, and no staining of the apical cells in the upper third (Fig. 1). Hence, the three groups (basal, middle, and upper layer) were defined for further analyses of terminal cell differentiation in NNSE. Two invasive cervical squamous cell carcinomas displayed strong BCL2 staining (SCC BCL2$^+$, Fig. 1) whereas two other squamous cell carcinomas showed no staining (SCC BCL2$^-$, Fig. 1).

Radial positions of chromosome 18 territory and BCL2 alleles in normal cervical squamous epithelium

First, the relative radial positions of chromosome 18 territories and the *BCL2* domains were determined in reference to the nuclear center in the three different layers of NNSE. In Table 1 the mean values and standard deviations are summarized. As shown in Fig. 4 and schematically illustrated in Fig. 6, chromosome 18 territories showed a general tendency (from the basal layer over the middle layer to the upper layer) for a shift towards the nuclear center. In those cell nuclei in which both homologues could be evaluated, objects with the smaller and larger distances to the nuclear center were analyzed separately since their locations were always significantly different (Tables 2, 3). Between the respective inner territory 18 and the outer territory the greatest difference was found in the basal layer whereas the smallest difference was found in the upper layer.

Evaluation of the relative radial distances of the *BCL2* gene domains revealed a tendency for a slight shift towards the center, following in general the chromosome 18 territories. Interestingly, after separate evaluation of inner and outer allele, greatest difference again was observed in the basal layer (Fig. 4), where the inner *BCL2* domain showed an orientation towards the nuclear center. Although the absolute values suggest this tendency, these changes did not reach high statistical significance.

In contrast to all other comparisons, the difference between the outer *BCL2* allele in the basal layer and the outer *BCL2* allele in the upper layer was statistically significant (Table 2) using the double-sided Kolmogorov–Smirnov test. This indicates a shift of the outer *BCL2* alleles towards the nuclear center, parallel to a decrease of gene expression during terminal cell differentiation.

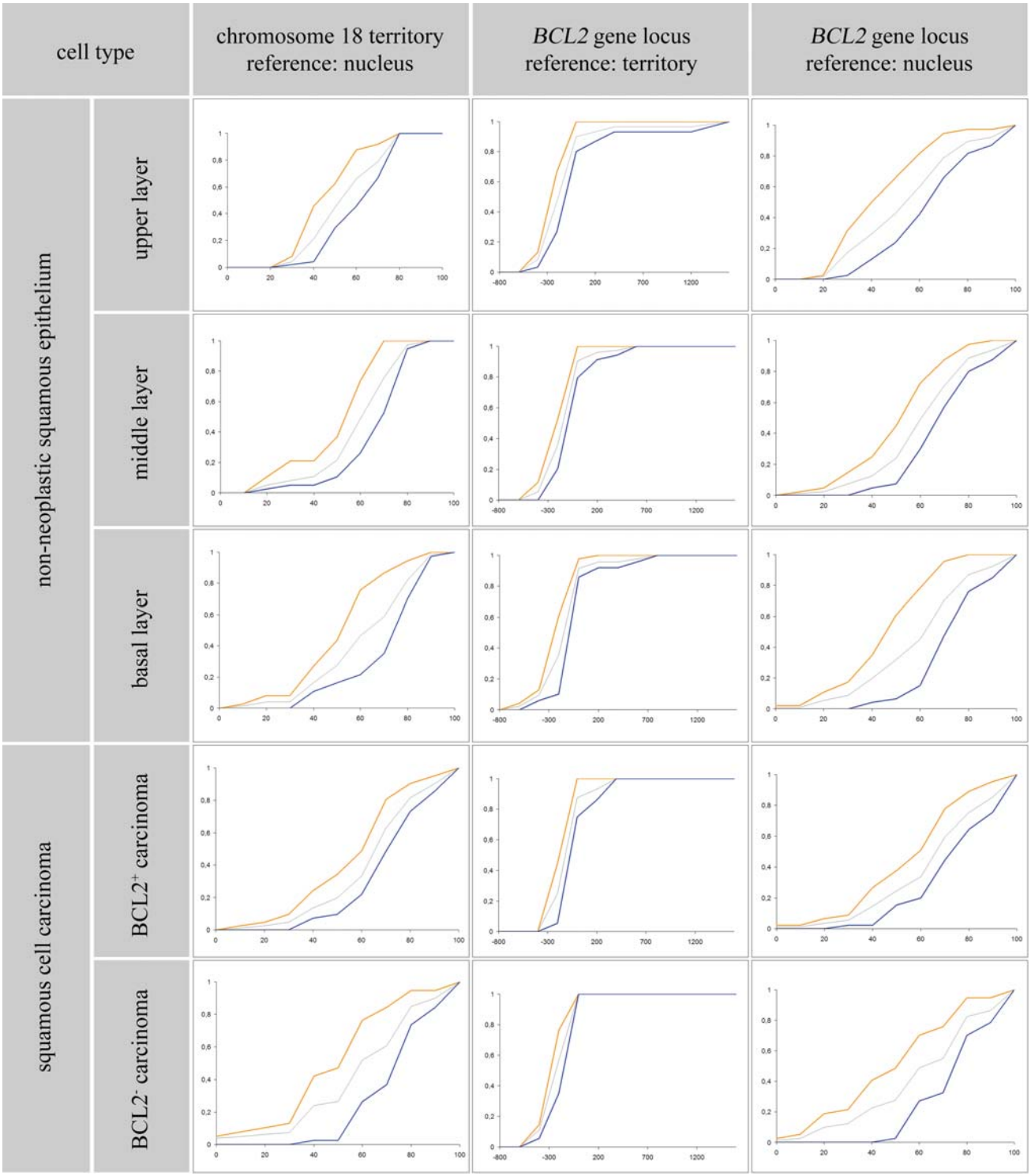

Fig. 4 Normalized cumulative frequency of labeled objects in the different nonneoplastic and neoplastic cell types (*rows*). The first column shows the normalized cumulative frequency of the relative radial position (percentage of the long nuclear main axis) of the chromosome 18 territories in reference to the nuclear center (0 on the *x*-axis). The second column shows the normalized cumulative frequency of the radial distances of the *BCL2* genes in nanometers (*x*-axis) with reference to the territorial surface (0 on the *x*-axis); note that this is a fictitious surface given by segmented labeled site. Due to the open flexibility of the chromatin, the genes can also be located inside the territory (*negative values*). The third column displays the normalized cumulative frequency of the relative radial position (percentage of the long nuclear main axis) of the *BCL2* genes in reference to the nuclear center (0 on the *x*-axis). In all histograms the *grey curve* refers to all nuclear elements, the *blue* one to the ("*outer*") elements positioned closer to the nuclear periphery, and the *orange* one to the ("*inner*") elements positioned closer to the nuclear center

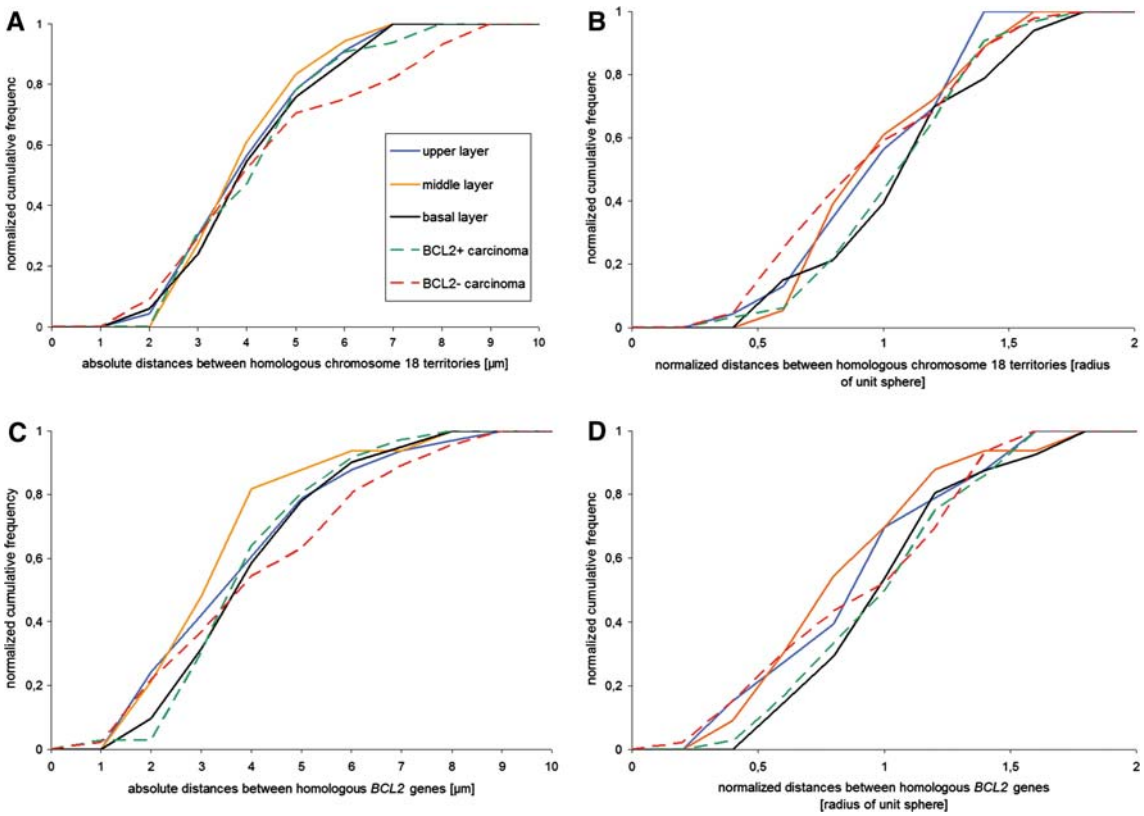

Fig. 5 Normalized cumulative frequency histograms of the absolute (**a**, **c**) and relative (**b**, **d**) distances of the homologous chromosome 18 territories (**a**, **b**) and homologous *BCL2* domains (**c**, **d**). Nonneoplastic squamous epithelium: *blue* upper layer, *orange* middle layer, *black* basal layer. Carcinomas: *dashed green*, SCC BCL2$^+$; *dashed red* SCC BCL2$^-$)

Within the limitations of the optical system used, the positions of the *BCL2* gene domains relative to the surface of the respective chromosome 18 territories were determined. No significant shift of the *BCL2* domains was observed (Fig. 4).

Radial positions of chromosome 18 territory and *BCL2* alleles in BCL2-positive and BCL2-negative cervical squamous cell carcinomas

As shown in Table 1 and Fig. 4 the difference of radial positions of both chromosome 18 territories was smaller in SCC BCL2$^+$ compared with SCC BCL2$^-$. The difference between the radial positions of the respective inner territories was significant, whereas the outer territories showed no significant position differences (Kolmogorov–Smirnov test, Table 2).

Comparison of the relative radial distances of the *BCL2* gene domains in reference to the nuclear center gives the impression that the inner *BCL2* allele was located more centrally and the outer allele slightly more peripherally in SCC BCL2$^-$ than in SCC BCL2$^+$ (Table 1; Fig. 4). However, this observation did not reach statistical significance (Table 3).

Determining the absolute radial distances of the *BCL2* gene domains to the chromosome 18 territorial surfaces showed that, in both BCL2$^+$ and BCL2$^-$ carcinoma cells, the two *BCL2* alleles were located on the surface of the territory (Fig. 4).

Comparison of radial positions of chromosome 18 territory and BCL2 alleles in cervical squamous cell carcinomas and nonneoplastic squamous epithelium

Regarding the radial positions of chromosome 18 territories in SCC compared with NNSE reveals that they were both located more peripherally in SCC BCL2$^+$ (Fig. 4; Table 1), reaching statistical significance, when compared with the upper layer of NNSE (Table 2). Interestingly, in separate analysis, only the inner territory was positioned significantly more peripherally in SCC BCL2$^+$ than in cells of the upper layer of NNSE. In contrast, in SCC BCL2$^-$ neither the inner nor the outer territories showed any significant differences compared with the upper layer of normal epithelium (Table 2).

When evaluating radial positions of the *BCL2* gene domains in SCC BCL2$^+$ and SCC BCL2$^-$, the gene domains appeared in general to be located more

Table 1 Radial nuclear positioning of chromosome 18 territories and *BCL2* gene domains, and distances of homologous elements

Relative radial positions of chromosome 18 territories (#18) in reference to the nuclear center (mean ± standard deviation, %)			
Cell type	#18 all	#18 inner	#18 outer
NNSE upper layer	59 ± 15	51 ± 14	67 ± 12
NNSE middle layer	64 ± 15	56 ± 15	73 ± 10
NNSE basal layer	66 ± 20	56 ± 18	76 ± 16
SCC $BCL2^+$	69 ± 20	62 ± 20	76 ± 16
SCC $BCL2^-$	64 ± 24	52 ± 23	77 ± 15
Relative radial positions of *BCL2* domains in reference to the nuclear center (mean ± standard deviation, %)			
Cell type	*BCL2* all	*BCL2* inner	*BCL2* outer
NNSE upper layer	59 ± 21	48 ± 18	69 ± 19
NNSE middle layer	65 ± 19	55 ± 18	74 ± 15
NNSE basal layer	63 ± 21	50 ± 18	77 ± 14
SCC $BCL2^+$	69 ± 22	60 ± 22	78 ± 18
SCC $BCL2^-$	65 ± 24	55 ± 26	80 ± 15

Absolute (μm) and relative distances (radius of the unit sphere of the territory) between the homologous chromosome 18 territories (#18) and *BCL2* domains

Cell type	#18 (abs.), μm	#18 (rel.)	*BCL2* (abs.), μm	*BCL2* (rel.)
NNSE upper layer	3.9 ± 1.4	0.9 ± 0.3	3.7 ± 1.8	0.9 ± 0.4
NNSE middle layer	3.8 ± 1.2	0.9 ± 0.3	3.3 ± 1.6	0.8 ± 0.4
NNSE basal layer	4.0 ± 1.4	1.1 ± 0.3	3.8 ± 1.6	1.0 ± 0.3
SCC $BCL2^+$	4.3 ± 1.5	1.1 ± 0.3	3.9 ± 1.5	1.0 ± 0.3
SCC $BCL2^-$	4.4 ± 2.1	0.9 ± 0.4	4.1 ± 2.1	0.9 ± 0.4

NNSE Nonneoplastic squamous epithelium, *SCC* squamous cell carcinoma

peripherally (Table 1) with statistical significance when compared with the upper layer of NNSE (Table 3). Of interest, in separate analysis, the inner *BCL2* allele in SCC $BCL2^+$ was positioned significantly more peripherally in comparison with the basal and upper layer of NNSE (Table 3; Fig. 4). In SCC $BCL2^-$ there was also a shift of the *BCL2* gene domains towards the nuclear periphery compared with normal epithelium, but in contrast to in SCC $BCL2^+$, only the outer allele showed a significant change in comparison with the upper layer of NNSE.

Analysis of *BCL2* gene domain positions in reference to the territorial surface in carcinoma revealed no significant differences in comparison with nonneoplastic epithelium, suggesting that, in both $BCL2^+$ and $BCL2^-$ carcinoma cells as well as in all layers of normal epithelium, both *BCL2* alleles were always located at the surface of chromosome 18 territory (Fig. 4).

Interchromosomal and interallelic distances

In addition to the radial positioning, the distances between the intensity barycenters of the homologous chromosome 18 territories and *BCL2* gene domains were measured (Table 1; Fig. 5). Besides the absolute distances in microns, also the relative distances after transformation of the cell nucleus to a unit sphere were considered. With the exception of the *BCL2* distance of the middle layer of NNSE in comparison with SCC $BCL2^-$ the absolute distance values showed no significant differences between the cell types analyzed. On average the homologue distances in the carcinomas were larger than in nonneoplastic epithelium. Comparing the absolute values of the *BCL2* domain distances with the chromosome 18 territory distances in nonneoplastic epithelium reflected the tendency of the gene orientation towards the nuclear center when BCL2 was not expressed. This was not supported by the two types of carcinomas.

In order to compare the distances without the influence of nuclear shape, the transformations to the unit sphere were analyzed. Since in the upper third the cells were highly flattened, leading to strong artificial rearrangements during transformation, they were excluded from this statistical evaluation. The relative distance of chromosome 18 territories in SCC $BCL2^+$ was significantly different from SCC $BCL2^-$. This was not observed for the *BCL2* gene domains, which is compatible with the allelic repositioning

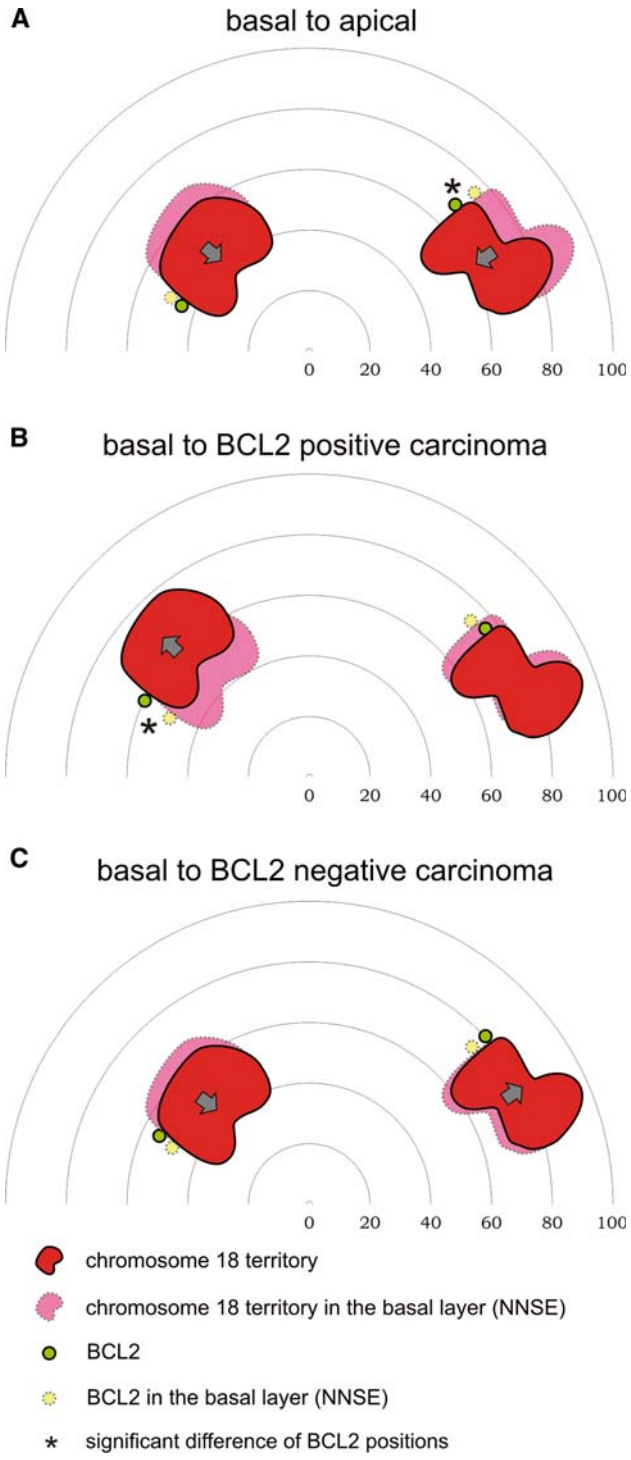

Fig. 6 Schematic depiction of the most important results. **a** Terminal cell differentiation: changes from basal to apical (upper layer) cells of nonneoplastic squamous epithelium. A shift of both chromosome 18 territories and both *BCL2* alleles towards the nuclear center was found, with a significantly different position (*asterisk*) of the outer chromosome 18 territory and *BCL2* allele. **b** Comparison of basal nonneoplastic cells with $BCL2^{+}$ carcinomas: the inner chromosome 18 territories and the inner *BCL2* gene domains (significant difference) are located more peripherally in the carcinomas, whereas the outer *BCL2* alleles and chromosome 18 territories are nearly at the same position in both cases. **c** Comparison of basal nonneoplastic cells with $BCL2^{-}$ carcinomas: the inner chromosome 18 territories are located slightly more centrally, whereas the outer chromosome 18 territories are nearly at the same position. The inner and outer *BCL2* alleles are positioned more peripherally without statistical significance

with gene expression (Table 4; Fig. 6). Slightly significant differences were also found between the basal and the middle layer of NNSE, supporting the same interpretation (Table 4).

Discussion

In order to evaluate changes of intranuclear gene domain positioning in reference to the nuclear center and to the territorial surfaces during terminal cell differentiation within the natural microanatomical context, we chose nonneoplastic cervical squamous epithelium (NNSE) as a model, in which cellular differentiation status correlates with the position of the cell in reference to the basement membrane. The apoptosis-related gene *BCL2* and its chromosome 18 territory were selected, because the different layers of squamous epithelium show clearly different protein expression levels in terms of a continuous strong expression of BCL2 in the basal layer, a weak expression in the middle layers, and no detectable expression in the upper layers. Furthermore, there are differences of BCL2 expression in the neoplastic counterpart—invasive cervical squamous cell carcinomas (SCC)—about half of which shows a BCL2 overexpression (54%), whereas others express little or no BCL2 (Ozalp et al. 2002). Analysis of the spatial distribution of *BCL2* genes, especially separate evaluation of the respective inner and outer *BCL2* allele and chromosome 18 territories, revealed interesting insights when comparing the three layers of NNSE, BCL2-overexpressing SCC, and BCL2-negative SCC.

The microanatomical context is assumed to be well preserved in formaldehyde-fixed, paraffin-wax-embedded tissues for the application of 3D FISH methods in analysis of genome architecture of the cell nucleus (Solovei et al. 2002). Unfortunately it is accompanied by the disadvantage of fixed cells, in contrast with cell cultures, which offer the opportunity for in vivo studies. This means that, in general, we cannot exclude fixation-induced changes of chromatin compaction which may show an influence on the nanoscale (Rauch et al. 2008). On the microsize scale of our measurements these changes should be negligible. On the other hand, tissue sections provide advantages of preserved tissue architecture, including extracellular structures and polarity.

In all NNSE and SCC cell groups both *BCL2* alleles were located on the surface of chromosome 18 territories,

Table 2 Statistical analysis of normalized chromosome 18 territory positioning in reference to the nuclear center: significance values (α values) for the double-sided Kolmogorov–Smirnov test

Overall analysis (no separation of the chromosomes)				
Cell type	SCC BCL2$^-$	SCC BCL2$^+$	NNSE basal layer	NNSE middle layer
NNSE upper layer	n.s.	0.006	n.s.	n.s.
NNSE middle layer	n.s.	n.s.	n.s.	
NNSE basal layer	n.s.	n.s.		
SCC BCL2$^+$	0.146			
Inner chromosome 18 territory				
Cell type	SCC BCL2$^-$	SCC BCL2$^+$	NNSE basal layer	NNSE middle layer
NNSE upper layer	n.s.	0.021	n.s.	n.s.
NNSE middle layer	n.s.	n.s.	n.s.	
NNSE basal layer	n.s.	n.s.		
SCC BCL2$^+$	0.079			
Outer chromosome 18 territory				
Cell type	SCC BCL2$^-$	SCC BCL2$^+$	NNSE basal layer	NNSE middle layer
NNSE upper layer	n.s.	n.s.	0.115	n.s.
NNSE middle layer	n.s.	n.s.	n.s.	
NNSE basal layer	n.s.	n.s.		
SCC BCL2$^+$	n.s.			
Inner versus outer chromosome 18 territory				
NNSE upper layer	NNSE middle layer	NNSE basal layer	SCC BCL2$^+$	SCC BCL2$^-$
0.026	0.022	<0.001	0.029	<0.001

NNSE Nonneoplastic squamous epithelium, *SCC* squamous cell carcinoma, *n.s.* not significant ($\alpha > 0.15$)

irrespective of their transcriptional activity. This was supported by results showing also independence of the territory surface gene location from gene activity (Cremer et al. 2004) especially in HeLa cell lines (Scheuermann et al. 2004). As a caveat it should be mentioned that these measurements were very close to the diffractive resolution limit of the objective lens used. A position on the territorial surface may facilitate regulatory interactions of the gene with proteins, noncoding RNAs, and genomic regions on other chromosomes. However, it has been shown that transcription is not confined to the territorial periphery (Mahy et al. 2002). Other transcriptionally active genes, which possibly do not need to be regulated to that extent, such as mouse β-globin, seem to be located more centrally within its territory (Brown et al. 2001, reviewed in Lanctôt et al. 2007). Interestingly, Gandhi et al. described that gene loci involved in interchromosomal rearrangements were located closer to the periphery of chromosome territories than were loci involved in intrachromosomal rearrangements (Gandhi et al. 2009). Thus, a general location of *BCL2* gene loci at the territorial surface could be associated with the high prevalence of interchromosomal *BCL2* rearrangements in follicular lymphoma, although we did not include lymphocytes in our study.

Chromosome 18 territories and *BCL2* gene domains show a shift towards the nuclear center when evaluating NNSE along basal, middle, and upper layers in the direction of terminal cell differentiation. No statistical significance was obtained in the analysis without separation of the two homologous chromosomes or the two *BCL2* alleles. Separate evaluation revealed differences of relative radial position of the outer *BCL2* allele in the basal layer, being located more peripherally than the outer *BCL2* allele of the upper layer. Interestingly, the greatest difference of radial positions between the inner and outer allele was observed in the basal layer with the strongest BCL2 expression, which may reflect a release of stabilizing interactions with heterochromatin during activation of transcription, as suggested by Harmon and Sedat (Harmon and Sedat 2005). The inner allele, in contrast, did not show significant differences between the three layers. These results indicate a shift of the more peripheral *BCL2* allele towards the nuclear center in terminal cell differentiation. One could assume that these findings only reflect the higher

Table 3 Statistical analysis of normalized *BCL2* gene domain positioning in reference to the nuclear center: significance values (α values) for the double-sided Kolmogorov–Smirnov test

Overall analysis (no separation of *BCL2* alleles)				
Cell type	SCC $BCL2^-$	SCC $BCL2^+$	NNSE basal layer	NNSE middle layer
NNSE upper layer	0.012	0.006	n.s.	0.133
NNSE middle layer	n.s.	n.s.	n.s.	
NNSE basal layer	n.s.	n.s.		
SCC $BCL2^+$	n.s.			
Inner *BCL2* allele				
Cell type	SCC $BCL2^-$	SCC $BCL2^+$	NNSE basal layer	NNSE middle layer
NNSE upper layer	n.s.	0.041	n.s.	n.s.
NNSE middle layer	n.s.	n.s.	n.s.	
NNSE basal layer	n.s.	0.065		
SCC $BCL2^+$	n.s.			
Outer *BCL2* allele				
Cell type	SCC $BCL2^-$	SCC $BCL2^+$	NNSE basal layer	NNSE middle layer
NNSE upper layer	0.041	n.s.	0.099	n.s.
NNSE middle layer	n.s.	n.s.	n.s.	
NNSE basal layer	n.s.	n.s.		
SCC $BCL2^+$	n.s.			
Inner versus outer *BCL2* allele				
NNSE upper layer	NNSE middle layer	NNSE basal layer	SCC $BCL2^+$	SCC $BCL2^-$
0.002	0.001	<0.001	0.012	0.001

NNSE Nonneoplastic squamous epithelium, *SCC* squamous cell carcinoma, *n.s.* not significant ($\alpha > 0.15$)

proliferation status of the basal cells and are an artefact due to a higher percentage of cells being in the cell cycle. However, this would not explain the loss of spatial allelic imbalance in SCC, which also has a high proliferation index. Thus, we think that our findings may reflect a physiological mechanism of unequal positioning, which is impaired after neoplastic transformation.

The allelic differences of spatial organization in BCL2-expressing basal cells may also point to allelic differences of *BCL2* gene transcription. Although a parenteral allele-specific expression in terms of imprinting has not been described for *BCL2* so far, this may be due to allelic imbalance of transcriptional activity or random monoallelic expression, such as is known for some other autosomal genes [reviewed in (Watanabe and Barlow 1996; Yang and Kuroda 2007)], for example, odorant receptor genes of murine olfactory neurons (Chess et al. 1994).

If transcriptional preponderance of one *BCL2* allele is hypothesized, the significance of the outer allele, being located more peripherally in basal cells compared with the upper ones, will point to the theory that the outer *BCL2* allele is the one that receives higher transcriptional activity. This hypothesis is further supported by the results of the analysis of radial *BCL2* positions in carcinoma: the inner allele in $BCL2^+$ (but not in $BCL2^-$) carcinoma cells was located significantly more peripherally compared with the basal nonneoplastic cells. This finding supports the theory that the more peripheral *BCL2* allele may represent the transcriptionally more active one.

This is in contrast to findings of several other investigators, who describe a relocation of activated genes towards the nuclear interior (Kosak et al. 2002; Lanctôt et al. 2007; Zink et al. 2004) and is also inconsistent with the assumption that the nuclear periphery is a compartment of general transcriptional inactivity. So far a causal link between chromatin mobility and gene expression remains to be established, and a main question is whether spatial genome organization affects or just reflects gene function (Fraser and Bickmore 2007). Most insights into such mechanisms may support the finding that gene silencing occurs at the nuclear periphery as a result of decreased chromatin mobility.

However, as shown by Casolari et al. in *S. cerevisiae*, gene activation can be associated with repositioning

Table 4 Statistical analysis of normalized homologue distances: significance values (α values) for the double-sided Kolmogorov–Smirnov test

Chromosome 18 territories				
Cell type	SCC BCL2$^-$	SCC BCL2$^+$	NNSE basal layer	NNSE middle layer
NNSE upper layer	Excluded	Excluded	Excluded	Excluded
NNSE middle layer	n.s.	0.121	0.139	
NNSE basal layer	0.124	n.s.		
SCC BCL2$^+$	0.072			
BCL2 genes				
Cell type	SCC BCL2$^-$	SCC BCL2$^+$	NNSE basal layer	NNSE middle layer
NNSE upper layer	Excluded	Excluded	Excluded	Excluded
NNSE middle layer	n.s.*	n.s.	0.121	
NNSE basal layer	n.s.	n.s.		
SCC BCL2$^+$	n.s.			

NNSE Nonneoplastic squamous epithelium, *SCC* squamous cell carcinoma, *n.s.* not significant ($\alpha > 0.15$)

* The absolute distances differ significantly ($\alpha = 0.051$)

towards the nuclear periphery in spatial proximity to nuclear pores (Casolari et al. 2004), which interact with promoters of genes in yeast (Schmid et al. 2006). The observation of the association of an activated locus with the nuclear periphery is neither sufficient nor necessary for the activity but serves to optimally express the gene (Taddei et al. 2006). Furthermore, even in mammals a general rule of gene relocation towards the nuclear interior or exterior in association with transcriptional activity seems to be inexistent, as illustrated by several other inconsistent findings (Hewitt et al. 2004; Ragoczy et al. 2006; Williams et al. 2006). Thus an attractive hypothesis may be that a gene locus can move into a favorable place within the nuclear architecture for optimized regulatory processes such as activation or repression. Activation of a gene means alteration of local chromatin structure for changes in accessibility. Since the intranuclear mobility of a gene locus is affected by its chromatin compaction, the locus becomes increasingly mobile with activation and finds a functional compartment that best supports its functional status. In this view, diffusional movements of gene loci are a critical property of gene expression and allow the loci to find ideal nuclear environments to be optimally expressed. This environment may not always be located in the nuclear center but also at the nuclear periphery when nuclear pore interactions may support the gene function (Soutoglou and Misteli 2007; Akhtar and Gasser 2007).

Thus, our findings appear to be still reasonable, with the consequence that gene regulation and gene loci movements have to be studied more intensively for many different types of genes in order to find appropriate rules. Chromosome 18, as a chromosome of very low gene density, may act quite differently as compared with chromosomes of high gene density, for instance, chromosome 19. It was shown that in proliferating cells chromosome 18 territories were generally located more peripherally (Bolzer et al. 2005; Bridger et al. 2000). The more peripheral location of chromosome 18 in carcinoma cells as compared with in normal cells was also found by Cremer et al. (2003), who compared HeLa cells (derived from cervix carcinoma) with normal cervical epithelium.

In addition, our findings may reflect a regulatory mechanism in BCL2-expressing NNSE cells, which leads to an allelic difference of nuclear positioning, and is probably associated with allelic differences of transcriptional activity. This mechanism, whatever it is, seems to be lost in neoplastic transformation, a phenomenon which may be comparable to loss of imprinting in cancer [reviewed in (Jelinic and Shaw 2007)]. Recently, an allelic imbalance in gene expression of eight genes, including *BCL2*, has been detected by evaluating relative expression levels of two single-nucleotide polymorphism (SNP) alleles in cancer cells (Milani et al. 2007). Allelic imbalance of gene expression may be a common finding in nonneoplastic cells, possibly representing a regulatory mechanism, which may be changed in cancer.

Although our observation of changes in nuclear genome organization may support the view of the nucleus as a self-organizing system in which regulatory processes drive the interactions and orientations of functional elements (Misteli 2008), this issue has not been investigated sufficiently yet. Further studies are needed to investigate associations between spatial allelic imbalances, epigenetic features, and allelic imbalances of gene expression, in order to elucidate mechanisms of gene regulation in nonneoplastic cells and its changes in neoplastic cells. This may help to uncover

possible regulatory factors, which also promote spatial relocation of genomic regions and may therefore be important in early carcinogenesis. From this point of view quantitative analysis of the 3D location of genes during carcinogenesis implemented in appropriate databases, e.g., accessible on a computing grid, might be a helpful tool in research and medical applications.

Acknowledgments The authors thank Prof. Dr. Rainer Siebert, Institute of Human Genetics, University Hospital Schleswig-Holstein, Kiel, Germany for providing the *BCL2* FISH probe and Mrs. Lieselotte Bokla for excellent technical assistance. The authors are also indebted to Prof. Dr. Christoph Cremer, Kirchhoff Institute of Physics, University of Heidelberg for his continuous support and stimulating discussions. Funding of the German Ministry of Education and Research (FKZ 13N8350 "COMBO-FISH" and FKZ 01IG07015G "Services@MediGRID") to Michael Hausmann is gratefully acknowledged. Finally, stimulations of Prof. Dr. Paul I. Prinz Zippl, University of Vienna, Austria, are acknowledged.

Conflict of interest statement The authors declare that they have no conflict of interest.

References

Abney JR, Cutler B, Fillbach ML et al (1997) Chromatin dynamics in interphase nuclei and its implications for nuclear structure. J Cell Biol 137:1459–1468. doi:10.1083/jcb.137.7.1459

Adams JM, Cory S (2007) The Bcl-2 apoptotic switch in cancer development and therapy. Oncogene 26:1324–1337. doi:10.1038/sj.onc.1210220

Akhtar A, Gasser SM (2007) The nuclear envelope and transcriptional control. Nat Rev Genet 8:507–517. doi:10.1038/nrg2122

Albiez H, Cremer M, Tiberi C et al (2006) Chromatin domains and the interchromatin compartment form structurally defined and functionally interacting nuclear networks. Chromosome Res 14:707–733. doi:10.1007/s10577-006-1086-x

Bartova E, Kozubek S, Jirsova P et al (2002) Nuclear structure and gene activity in human differentiated cells. J Struct Biol 139:76–89. doi:10.1016/S1047-8477(02)00560-9

Bolzer A, Kreth G, Solovei I et al (2005) Three-dimensional maps of all chromosomes in human male fibroblast nuclei and prometaphase rosettes. PLoS Biol 3:e157. doi:10.1371/journal.pbio.0030157

Branco MR, Pombo A (2006) Intermingling of chromosome territories in interphase suggests role in translocations and transcription-dependent associations. PLoS Biol 4:e138. doi:10.1371/journal.pbio.0040138

Bridger JM, Boyle S, Kill IR et al (2000) Re-modelling of nuclear architecture in quiescent and senescent human fibroblasts. Curr Biol 10:149–152. doi:10.1016/S0960-9822(00)00312-2

Brown KE, Amoils S, Horn JM et al (2001) Expression of alpha- and beta-globin genes occurs within different nuclear domains in haemopoietic cells. Nat Cell Biol 3:602–606. doi:10.1038/35078577

Casolari JM, Brown CR, Komili S et al (2004) Genome-wide localization of the nuclear transport machinery couples transcriptional status and nuclear organization. Cell 117:427–439. doi:10.1016/S0092-8674(04)00448-9

Chess A, Simon I, Cedar H et al (1994) Allelic inactivation regulates olfactory receptor gene expression. Cell 78:823–834. doi:10.1016/S0092-8674(94)90562-2

Cory S, Adams JM (2002) The Bcl2 family: regulators of the cellular life-or-death switch. Nat Rev Cancer 2:647–656. doi:10.1038/nrc883

Cremer T, Cremer C (2001) Chromosome territories, nuclear architecture and gene regulation in mammalian cells. Nat Rev Genet 2:292–301. doi:10.1038/35066075

Cremer T, Kreth G, Koester H et al (2000) Chromosome territories, interchromatin domain compartment, and nuclear matrix: an integrated view of the functional nuclear architecture. Crit Rev Eukaryot Gene Expr 10:179–212

Cremer M, Kupper K, Wagler B et al (2003) Inheritance of gene density-related higher order chromatin arrangements in normal and tumor cell nuclei. J Cell Biol 162:809–820. doi:10.1083/jcb.200304096

Cremer T, Kupper K, Dietzel S et al (2004) Higher order chromatin architecture in the cell nucleus: on the way from structure to function. Biol Cell 96:555–567. doi:10.1016/j.biolcel.2004.07.002

Cremer T, Cremer M, Dietzel S et al (2006) Chromosome territories—a functional nuclear landscape. Curr Opin Cell Biol 18:307–316. doi:10.1016/j.ceb.2006.04.007

Cremer M, Grasser F, Lanctôt C et al (2008) multicolour 3D fluorescence in situ hybridization for imaging interphase chromosomes. Methods Mol Biol 463:205–239. doi:10.1007/978-1-59745-406-3_15

Dundr M, Ospina JK, Sung MH et al (2007) Actin-dependent intranuclear repositioning of an active gene locus in vivo. J Cell Biol 179:1095–1103. doi:10.1083/jcb.200710058

Fraser P, Bickmore W (2007) Nuclear organization of the genome and the potential for gene regulation. Nature 447:413–417. doi:10.1038/nature05916

Gandhi MS, Stringer JR, Nikiforova MN et al (2009) Gene position within chromosome territories correlates with their involvement in distinct rearrangement types in thyroid cancer cells. Genes Chromosomes Cancer 48:222–228. doi:10.1002/gcc.20639

Hagemann T, Bozanovic T, Hooper S et al (2007) Molecular profiling of cervical cancer progression. Br J Cancer 96:321–328. doi:10.1038/sj.bjc.6603543

Harmon B, Sedat J (2005) Cell-by-cell dissection of gene expression and chromosomal interactions reveals consequences of nuclear reorganization. PLoS Biol 3:e67. doi:10.1371/journal.pbio.0030067

Hewitt SL, High FA, Reiner SL et al (2004) Nuclear repositioning marks the selective exclusion of lineage-inappropriate transcription factor loci during T helper cell differentiation. Eur J Immunol 34:3604–3613. doi:10.1002/eji.200425469

Jelinic P, Shaw P (2007) Loss of imprinting and cancer. J Pathol 211:261–268. doi:10.1002/path.2116

Kosak ST, Groudine M (2004) Form follows function: the genomic organization of cellular differentiation. Genes Dev 18:1371–1384. doi:10.1101/gad.1209304

Kosak ST, Skok JA, Medina KL et al (2002) Subnuclear compartmentalization of immunoglobulin loci during lymphocyte development. Science 296:158–162. doi:10.1126/science.1068768

Kosak ST, Scalz D, Alworth SV et al (2007) Coordinate gene regulation during hematopoiesis is related to genomic organization. PLoS Biol 5:e309. doi:10.1371/journal.pbio.0050309

Kozubek S, Lukasova E, Jirsova P et al (2002) 3D Structure of the human genome: order in randomness. Chromosoma 111:321–331. doi:10.1007/s00412-002-0210-8

Kupper K, Kolbi A, Biener D et al (2007) Radial chromatin positioning is shaped by local gene density, not by gene expression. Chromosoma 116:285–306. doi:10.1007/s00412-007-0098-4

Lanctôt C, Cheutin T, Cremer M et al (2007) Dynamic genome architecture in the nuclear space: regulation of gene expression

in three dimensions. Nat Rev Genet 8:104–115. doi:10.1038/nrg2041

Lelievre SA, Weaver VM, Nickerson JA et al (1998) Tissue phenotype depends on reciprocal interactions between the extracellular matrix and the structural organization of the nucleus. Proc Natl Acad Sci USA 95:14711–14716. doi:10.1073/pnas.95.25.14711

Mahy NL, Perry PE, Gilchrist S et al (2002) Spatial organization of active and inactive genes and noncoding DNA within chromosome territories. J Cell Biol 157:579–589. doi:10.1083/jcb.200111071

Milani L, Gupta M, Andersen M et al (2007) Allelic imbalance in gene expression as a guide to cis-acting regulatory single nucleotide polymorphisms in cancer cells. Nucleic Acids Res 35:e34. doi:10.1093/nar/gkl1152

Misteli T (2008) Nuclear order out of chaos. Nature 456:333–334. doi:10.1038/456333a

Neusser M, Schubel V, Koch A et al (2007) Evolutionarily conserved, cell type or species specific higher order chromatin arrangements in interphase nuclei of primates. Chromosoma 116:307–320. doi:10.1007/s00412-007-0099-3

Ozalp SS, Yalcin OT, Tanir HM et al (2002) Bcl-2 expression in preinvasive and invasive cervical lesions. Eur J Gynaecol Oncol 23:419–422

Parada LA, McQueen PG, Munson PJ et al (2002) Conservation of relative chromosome positioning in normal and cancer cells. Curr Biol 12:1692–1697. doi:10.1016/S0960-9822(02)01166-1

Ragoczy T, Bender MA, Telling A et al (2006) The locus control region is required for association of the murine beta-globin locus with engaged transcription factories during erythroid maturation. Genes Dev 20:1447–1457. doi:10.1101/gad.1419506

Rauch J, Knoch TA, Solovei I et al (2008) Light optical precision measurements of the active and inactive Prader-Willi syndrome imprinted regions in human cell nuclei. Differentiation 76:66–82

Scheuermann MO, Tajbakhsh J, Kurz A et al (2004) Topology of genes and nontranscribed sequences in human interphase nuclei. Exp Cell Res 301:266–279. doi:10.1016/j.yexcr.2004.08.031

Schmid M, Arib G, Laemmli C et al (2006) Nup-PI: the nucleopore-promoter interaction of genes in yeast. Mol Cell 21:379–391. doi:10.1016/j.molcel.2005.12.012

Sexton T, Schober H, Fraser P et al (2007) Gene regulation through nuclear organization. Nat Struct Mol Biol 14:1049–1055. doi:10.1038/nsmb1324

Sobin LH, Wittekind C (2002) TNM classification of malignant tumours. Wiley, New York

Sokal RR, Rohlf FJ (1981) Biometry. W.H. Freeman, New York, pp 440–445

Solovei I, Cavallo A, Schermelleh L et al (2002) Spatial preservation of nuclear chromatin architecture during three-dimensional fluorescence in situ hybridization (3D-FISH). Exp Cell Res 276:10–23. doi:10.1006/excr.2002.5513

Soutoglou E, Misteli T (2007) Mobility and immobility of chromatin in transcription and genome stability. Curr Opin Genet Dev 17:435–442. doi:10.1016/j.gde.2007.08.004

Stein S (2006) Quantifizierung der dreidimensionalen Mikroarchitektur von Genomelementen nach spezifischer Fluoreszenzmarkierung in fixierten und vitalen Zellen. Ph.D. Thesis, Faculty of Physics and Astronomy, University of Heidelberg

Taddei A, Van Houwe G, Hediger F et al (2006) Nuclear pore association confers optimal expression levels for an inducible yeast gene. Nature 441:774–778. doi:10.1038/nature04845

Tanabe H, Habermann FA, Solovei I et al (2002) Non-random radial arrangements of interphase chromosome territories: evolutionary considerations and functional implications. Mutat Res 504:37–45. doi:10.1016/S0027-5107(02)00077-5

Watanabe D, Barlow DP (1996) Random and imprinted monoallelic expression. Genes Cells 1:795–802. doi:10.1046/j.1365-2443.1996.d01-276.x

Wells M, Östor AG, Crum CP (2003) Epithelial tumours. In: Tavassoli FA, Devilee P (eds) Pathology and genetics of tumours of the breast and female genital organs. IARC press, Lyon, pp 262–279

Wiech T, Timme S, Riede F et al (2005) Human archival tissues provide a valuable source for the analysis of spatial genome organization. Histochem Cell Biol 123:229–238. doi:10.1007/s00418-005-0768-3

Williams RR, Azuara V, Perry P et al (2006) Neural induction promotes large-scale chromatin reorganisation of the Mash1 locus. J Cell Sci 119:132–140. doi:10.1242/jcs.02727

Yang PK, Kuroda MI (2007) Noncoding RNAs and intranuclear positioning in monoallelic gene expression. Cell 128:777–786. doi:10.1016/j.cell.2007.01.032

Youn CK, Cho HJ, Kim SH et al (2005) Bcl-2 expression suppresses mismatch repair activity through inhibition of E2F transcriptional activity. Nat Cell Biol 7:137–147. doi:10.1038/ncb1215

Zink D, Cremer T, Saffrich R et al (1998) Structure and dynamics of human interphase chromosome territories in vivo. Hum Genet 102:241–251. doi:10.1007/s004390050686

Zink D, Amaral MD, Englmann A et al (2004) Transcription-dependent spatial arrangements of CFTR and adjacent genes in human cell nuclei. J Cell Biol 166:815–825. doi:10.1083/jcb.200404107